Acta Cryst E CRYSTALLOGRAPHIC COMMUNICATIONS

ISSN 2056-9890

Synthesis, crystal structure determination, Hirshfeld surface and crystal void analyses, interaction energy calculations and energy frameworks of *N*-(2-methylphenyl)-*N*′-pivaloylthiourea

Sharatha Kumar[a]* and Tuncer Hökelek[b]

[a]Department of Chemistry, Yenepoya Institute of Arts, Science, Commerce and Management, Mangaluru, Yenepoya University (Deemed to be university), 575013 Karnataka, India, and [b]Hacettepe University, Department of Physics, 06800 Beytepe-Ankara, Türkiye. *Correspondence e-mail: sharathyiascm@yenepoya.edu.in

Received 4 August 2026
Accepted 26 August 2026

Edited by M. Weil, Vienna University of Technology, Austria

Keywords: crystal structure; pivaloyl; thiourea-derivative; 2-methylphenyl substituent; intermolecular interactions.

CCDC reference: 1816816

Supporting information: this article has supporting information at journals.iucr.org/e

The title compound [systematic name: 3-(2,2-dimethylpropanoyl)-1-(2-methylphenyl)thiourea], $C_{13}H_{18}N_2OS$, consists of methylphenyl and pivaloyl moieties attached to the N atoms of thiourea. The latter is twisted by 78.08 (10)° with respect to the phenyl ring. An intramolecular N—H···O hydrogen bond with an *S*(6) ring motif consolidates the molecular conformation. In the crystal, C—H···S hydrogen bonds link two molecules, enclosing $R_2^2(14)$ ring motifs, into centrosymmetric dimers. Furthermore, π–π stacking and C—H···π(ring) interactions are present. Hirshfeld surface analysis revealed that the most important contributions to the crystal packing are from H···H (62.4%), H···S/S···H (13.6%) and H···C/C···H (12.9%) interactions. The volume of the crystal voids and the percentage of free space were calculated to be 91.57 Å^3 and 13.35%, showing that there is no large cavity in the crystal packing. A C—H···S hydrogen-bonding energy of −5.4 kJ mol^{-1} was calculated. Evaluation of the electrostatic, dispersion and total energy frameworks indicates that the packing is dominated by dispersion energy contributions.

1. Chemical context

N-substituted *N*-acylthioureas are important synthetic intermediates for the preparation of a variety of heterocyclic compounds through cyclization reactions (Saeed *et al.*, 2016; Aly *et al.*, 2016). They have also attracted considerable interest as precursors for anion receptors (Blažek Bregovic *et al.*, 2015; Zhang *et al.*, 2006), organocatalysts (Guang *et al.*, 2015; Mao *et al.*, 2013; Saeed *et al.*, 2017), corrosion inhibitors (Al-Abbassi *et al.*, 2023), and non-ionic surfactants (Ullah *et al.*, 2015). Moreover, numerous acylthiourea derivatives exhibit a broad spectrum of biological activities, including anticonvulsant (Bielenica *et al.*, 2016), anticancer (Ruswantor *et al.*, 2015; Kumar & Chimni, 2015; Ribeiro *et al.*, 2023), antidiabetic (Faidullah *et al.*, 2011), anti-inflammatory (Canatar *et al.*, 2023; Mohamed *et al.*, 2021), anti-HIV (Singh & Ganguly, 2018), antimicrobial (Zhong *et al.*, 2008; Aher *et al.*, 2009), urease inhibitory (Khan *et al.*, 2014), herbicidal (Xu *et al.*, 2003*a*), and insecticidal (Xu *et al.*, 2003*b*) activities. Thiourea derivatives containing sulfur- and nitrogen-donor atoms have also attracted considerable attention in medicinal chemistry owing to their interesting pharmacological properties. In particular, thiourea-based compounds have been investigated as aromatase inhibitors for the treatment of estrogen-dependent breast cancer (Pingaew *et al.*, 2018). Their anticancer activity has also been attributed to interference with microtubule assemblies, leading to mitotic arrest and subsequent cell death (Anchoori

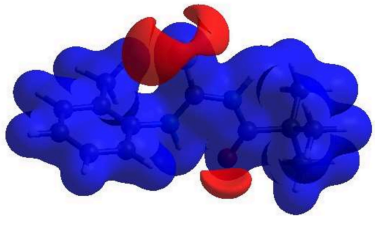

et al., 2008). Moreover, several N-substituted phenylthioureas inhibit tyrosinase-mediated melanogenesis and have shown promising activity against melanoma and other hyperpigmentation disorders (Thanigaimalai *et al.*, 2011).

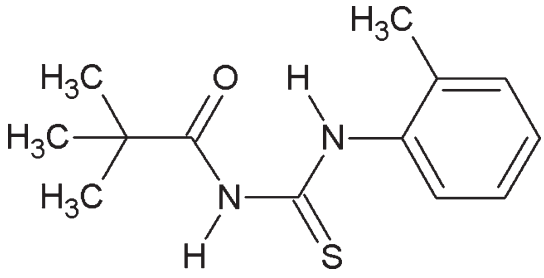

In the context given above, we studied the molecular and crystal structures of the title compound (**I**) and also carried out Hirshfeld surface (HS) and crystal void analyses and calculations of its interaction energy and energy frameworks.

2. Structural commentary

Compound (**I**) consists of methylphenyl and pivaloyl moieties attached to the N atoms of the central thiourea group (Fig. 1). An intramolecular N—H···O hydrogen bond (Table 1) with an *S*(6) ring motif (Etter *et al.*, 1990) stabilizes the molecular conformation (Fig. 2).

The planar (O1/C8/C9/C12) and thiourea (S1/C7/N1/N2) fragments [root-mean-square deviations of 0.017 (3) and 0.002 (2) Å, respectively] subtend a dihedral angle of 3.9 (1)°. The O1, C8, C9 and C12 atoms are 0.049 (2), −0.004 (3), −0.079 (3) and 0.037 (4) Å, respectively, away from the least-squares plane of the thiourea group. The dihedral angles between the phenyl (C1–C6) ring and the (O1/C8/C9/C12) and thiourea groups are 81.88 (13) and 78.08 (10)°, respectively. The C13 and N1 atoms are 0.061 (5) and 0.008 (3) Å away from the least-squares plane of the phenyl ring.

The bond lengths (Allen *et al.*, 1987) and angles in the entire molecule are in normal ranges and comparable to those in similar compounds; for a detailed comparison, see Section 4.

Table 1
Hydrogen-bond geometry (Å, °).

*Cg*1 is the centroid of the C1–C6 ring.

D—H···*A*	*D*—H	H···*A*	*D*···*A*	*D*—H···*A*
N1—H1*N*···O1	0.84 (2)	1.98 (3)	2.644 (3)	135 (3)
C11—H11*A*···S1^{i}	0.96	2.79	3.663 (4)	152
C12—H12*C*···*Cg*1^{ii}	0.96	2.92	3.640 (5)	133

Symmetry codes: (i) $-x+1, -y+1, -z+1$; (ii) $-x+2, -y, -z+1$.

3. Supramolecular features

In the crystal, weak C—H···S hydrogen bonds (Table 1) link the molecules, enclosing $R_2^2(14)$ ring motifs (Etter *et al.*, 1990), into centrosymmetric dimers (Fig. 2). Furthermore, C—H···π(ring) interactions (Table 1) and weak π–π stacking interactions between parallel phenyl rings, with centroid-to-centroid distance of 4.134 (2) Å [dihedral angle α = 0.0 (2)° and slippage = 2.288 Å], help to consolidate the packing.

The intermolecular interactions in the crystal were quantified by a Hirshfeld surface (HS) analysis using *CrystalExplorer* (Spackman *et al.*, 2021). Fig. 3 shows the HS mapped over

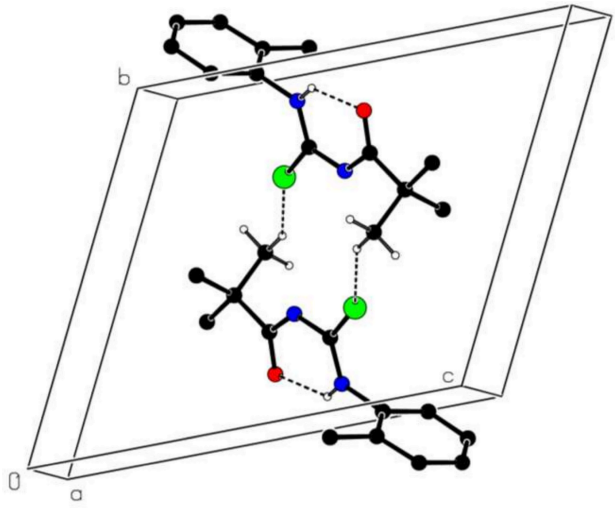

Figure 2
A partial packing diagram of (**I**) viewed down the *a* axis showing the intramolecular N—H···O [*S*(6) ring motif] and intermolecular C—H···S hydrogen bonds [$R_2^2(14)$ ring motif] as dashed lines.

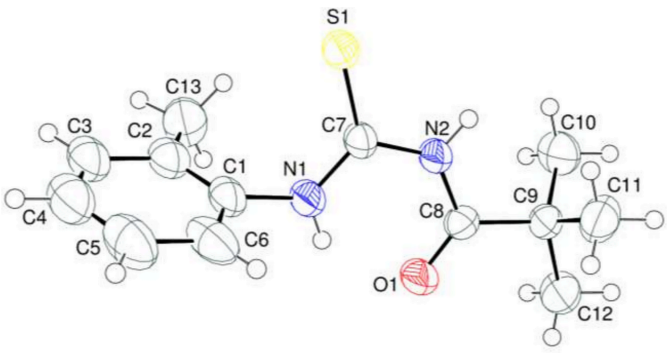

Figure 1
The molecular structure of (**I**) with displacement ellipsoids drawn at the 50% probability level.

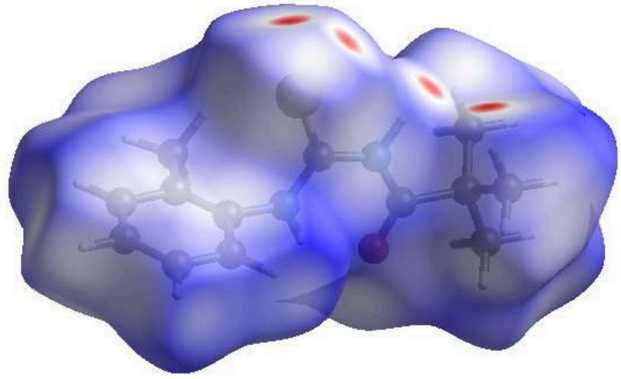

Figure 3
View of the three-dimensional Hirshfeld surface plotted over d_{norm}.

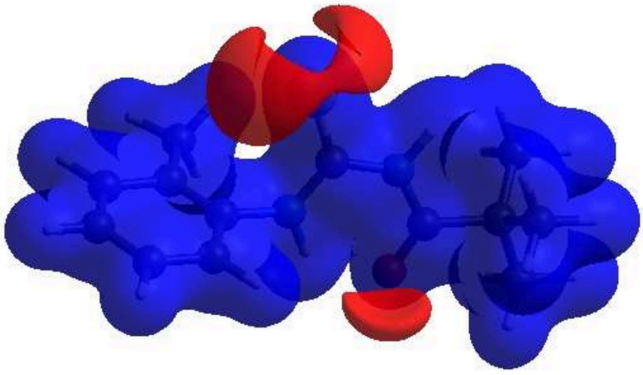

Figure 4
View of the three-dimensional Hirshfeld surface of (**I**) plotted over electrostatic potential using the STO-3 G basis set at the Hartree–Fock level of theory. Hydrogen-bond donors and acceptors are shown as blue and red regions around the atoms, corresponding to positive and negative potentials, respectively.

d_{norm} where the white surface indicates contacts with distances equal to the sum of van der Waals radii, and the red and blue colours indicate distances shorter (in close contact) or longer (distinct contacts) than the van der Waals radii, respectively. The red spots indicate their roles as the respective donors and/or acceptors atoms in hydrogen-bonding interaction, as discussed; they also appear as blue and red regions corresponding to positive and negative potentials on the HS mapped over electrostatic potential (Fig. 4), indicating positive (hydrogen-bond donors) and negative (hydrogen-bond acceptors) electrostatic potentials. The π–π stacking and the C—H···π(ring) interactions are indicated in Fig. 5*a* by the presence of adjacent red and blue triangles, and in Fig. 5*b* by the presence of red π-holes.

The overall two-dimensional fingerprint plot is shown in Fig. 6*a*, and those delineated into H···H, H···S/S···H, H···C/C···H, H···O/O···H, H···N/N···H and C···C interactions are illustrated in Fig. 6*b*–*g*, respectively, revealing that H···H, H···S/S···H and H···C/C···H contacts make the most significant contributions to the HS.

A void analysis of the crystal packing (Fig. 7) revealed the void volume and the percentage of free space in the unit cell to be 91.57 Å^3 and 13.35%, respectively, which indicates a rather compact packing of molecules in the crystal.

Intermolecular interaction energies were calculated using the CE–B3LYP/6–31G(d,p) energy model available in *Crys-*

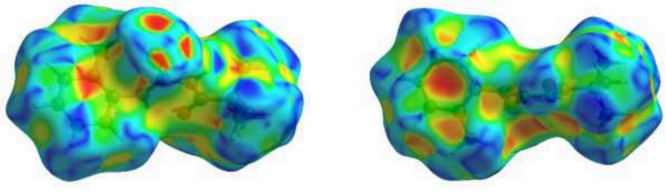

Figure 5
Two orientations of the shape-index, showing (*a*) the π–π and (*b*) the C—H···π(ring) interactions.

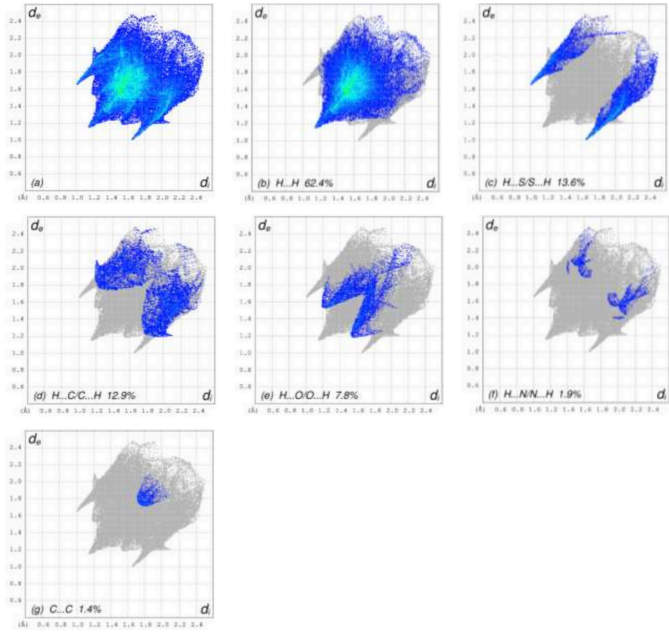

Figure 6
The full two-dimensional fingerprint plots of (**I**), showing (*a*) all interactions, and delineated into (*b*) H···H, (*c*) H···S/S···H, (*d*) H···C/C···H, (*e*) H···O/O···H, (*f*) H···N/N···H and (*g*) C···C interactions. The d_i and d_e values are the closest internal and external distances (in Å) from given points on the Hirshfeld surface.

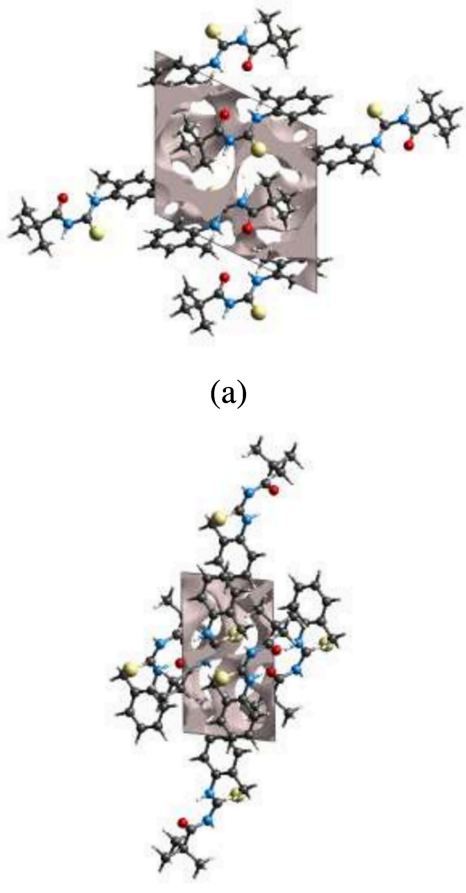

Figure 7
Crystal voids viewed down the (*a*) *a* axis and (*b*) *b* axis.

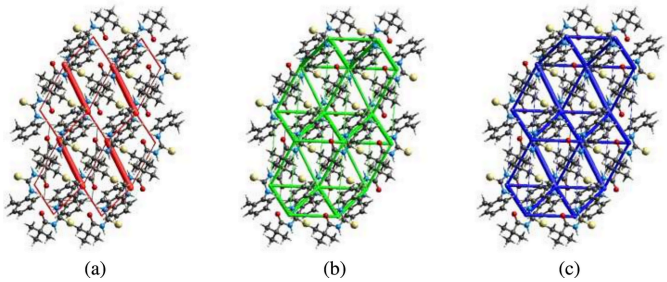

Figure 8
The energy frameworks for a cluster of molecules viewed down the *c* axis showing the (*a*) electrostatic energy, (*b*) dispersion energy and (*c*) total energy diagrams. The cylindrical radius is proportional to the relative strength of the corresponding energies and they were adjusted to the same scale factor of 80 with cut-off value of 5 kJ mol^{-1} within 2×2×2 unit cells.

talExplorer (Spackman *et al.*, 2021), where a cluster of molecules is generated by applying crystallographic symmetry operations with respect to a selected central molecule within the radius of 3.8 Å by default. The total intermolecular energy (E_{tot}) is the sum of electrostatic (E_{ele}), polarization (E_{pol}), dispersion (E_{dis}) and exchange-repulsion (E_{rep}) energies (Turner *et al.*, 2015) with scale factors of 1.057, 0.740, 0.871 and 0.618, respectively (Mackenzie *et al.*, 2017). Hydrogen-bonding interaction energies (in kJ mol^{-1}) were calculated to be −0.6 (E_{ele}), −0.3 (E_{pol}), −8.7 (E_{dis}), 4.9 (E_{rep}) and −5.4 (E_{tot}) for the C11—H11*A*···S1 hydrogen-bonding interaction.

Energy frameworks combine the calculation of intermolecular interaction energies with a graphical representation of their magnitudes, in which they were constructed for E_{ele} (red cylinders), E_{dis} (green cylinders) and E_{tot} (blue cylinders), as shown in Fig. 8*a*, *b* and *c*. The evaluation of the electrostatic, dispersion and total energy frameworks indicates that the stabilization in the crystal structure is dominated *via* the dispersion energy contributions.

Table 2
Experimental details.

Crystal data	
Chemical formula	$C_{13}H_{18}N_2OS$
M_r	250.35
Crystal system, space group	Triclinic, $P\overline{1}$
Temperature (K)	293
a, *b*, *c* (Å)	6.1050 (4), 10.7020 (3), 11.8910 (3)
α, β, γ (°)	63.290 (4), 81.600 (3), 84.340 (4)
V (Å^3)	686.08 (6)
Z	2
Radiation type	Mo *Kα*
μ (mm^{-1})	0.22
Crystal size (mm)	0.50 × 0.48 × 0.16
Data collection	
Diffractometer	Oxford Diffraction Xcalibur with Sapphire CCD Detector
Absorption correction	Multi-scan (*CrysAlis RED*; Oxford Diffraction, 2009)
T_{min}, T_{max}	0.897, 0.965
No. of measured, independent and observed [$I > 2\sigma(I)$] reflections	4335, 2756, 2287
R_{int}	0.010
$(\sin\theta/\lambda)_{max}$ (Å^{-1})	0.625
Refinement	
$R[F^2 > 2\sigma(F^2)]$, $wR(F^2)$, *S*	0.064, 0.164, 1.16
No. of reflections	2756
No. of parameters	160
No. of restraints	3
H-atom treatment	H atoms treated by a mixture of independent and constrained refinement
$\Delta\rho_{max}$, $\Delta\rho_{min}$ (e Å^{-3})	0.71, −0.24

Computer programs: *CrysAlis CCD* and *CrysAlis RED* (Oxford Diffraction, 2009), *SHELXT* (Sheldrick, 2015*a*), *SHELXL* (Sheldrick, 2015*b*) and *ORTEP-3 for Windows* and *WinGX* (Farrugia, 2012).

4. Database survey

A search of the Cambridge Structural Database (CSD, Version 6.00, updated May 2025; Groom *et al.*, 2016) revealed six structures closely related to *N*-(2-methylphenyl)-*N*′-pivaloylthiourea. These include 1-(3-nitrophenyl)-3-pivaloylthiourea, $C_{12}H_{15}N_3O_3S$ [CSD refcode RIZCUZ; (**II**) Yusof *et al.*, 2008], 1-(2-nitrophenyl)-3-pivaloylthiourea, $C_{12}H_{15}N_3O_3S$ [GINDEN; (**III**) Saeed & Flörke, 2007*a*], 1-(2,4-dichlorophenyl)-3-pivaloylthiourea, $C_{12}H_{14}Cl_2N_2OS$ [HIRDOC; (**IV**) Saeed & Flörke, 2007*b*], 1-(3-bromophenyl)-3-pivaloylthiourea, $C_{12}H_{15}BrN_2OS$ [CICREM; (**V**) Sultana *et al.*, 2007*a*], 1-(4-nitrophenyl)-3-pivaloylthiourea, $C_{12}H_{15}N_3O_3S$ [GIHFOT; (**VI**) Sultana *et al.*, 2007*b*] and 1-(3-chlorophenyl)-3-pivaloylthiourea, $C_{12}H_{15}ClN_2OS$ [WIHBAR; (**VII**) Shoukat *et al.*, 2007],

In the title compound (**I**), the C2—C1—C6 bond angle [122.8 (3)°] is wider than the corresponding ones in compounds (**II**)–(**VI**), and the N1—C7—N2 bond angle (116.4 (2)°) is also wider than those in compounds (**IV** – **VI**). On the other hand, the C1—N1—C7 bond angle [123.3 (2)°] is narrowed with respect to those in compounds (**III**), (**IV**) and (**VI**), and the S1—C7—N1 bond angle [124.4 (2)]) is also narrowed relative to those in compounds (**IV**) and (**VI**).

5. Synthesis and crystallization

Compound (**I**) was synthesized by adding a solution of pivaloyl chloride (0.10 mol) in acetone (30 ml) dropwise to a suspension of ammonium thiocyanate (0.10 mol) in acetone (30 ml). The resulting reaction mixture was stirred for 2 h, and then refluxed for 30 min. After cooling to room temperature, a solution of 2-methylaniline (0.10 mol) in acetone (10 ml) was added, and the reaction mixture was refluxed for 3 h. The progress of the reaction was monitored by thin-layer chromatography (TLC). Upon completion, the reaction mixture was poured into cold acidified water (5%$_{wt}$ HCl). The precipitated solid was collected by vacuum filtration, washed thoroughly with water, and dried. White solid, yield 82%, m.p. 371–373 K. IR (KBr) cm^{-1}: 3347 (N—H str.), 1179 (C═S str.) and 1681 (C═O str.). ^{1}H NMR (400 MHz, $CDCl_3$-d_6): δ (ppm) 12.03 (*s*, 1H), 8.50 (*s*, 1H), 7.25–7.62 (*m*, 4H, Ar-H 2-methylphenyl ring), 2.34 (*s*, 3H, CH_3), 1.30 [*s*, 9H, $(CH_3)_3$], ^{13}C NMR (400 MHz, $CDCl_3$-d_6): δ (ppm) 27.1, 21.0, 134.8, 124.3, 129.4, 136.9, 129.4, 121.3, 171.0, 178.4. Colourless crystals suitable for

single-crystal X-ray diffraction analysis were obtained by slow evaporation of an acetonitrile solution at room temperature.

6. Refinement

Crystal data, data collection and structure refinement details are summarized in Table 2. Three reflections were omitted from the final refinement cycles, and similarity restraints applied to some of the C atoms of the phenyl ring. Hydrogen atoms attached to the N atoms of thiourea were located from difference-Fourier maps and refined with a distance restraint of N—H = 0.86 (2) Å, and with U_{iso}(H) = 1.2U_{eq}(N). The C-bound hydrogen-atom positions were calculated geometrically at distances of 0.93 Å (aromatic) and 0.96 Å (methyl) and refined using a riding model.

Acknowledgements

The authors thank the Yenepoya Deemed to be University for the facilities and financial support. TH is also grateful to Hacettepe University Scientific Research Project Unit (Grant No. 013 D04 602 004).

References

Aher, N. G., Pore, V. S., Mishra, N. N., Kumar, A., Shukla, P. K., Sharma, A. & Bhat, M. K. (2009). *Bioorg. Med. Chem. Lett.* **19**, 759–763.

Al-Abbassi, A. A., Kayed, S. F. & Kassim, M. B. (2023). *Inorg. Chem. Commun.* **156**, 111155.

Allen, F. H., Kennard, O., Watson, D. G., Brammer, L., Orpen, A. G. & Taylor, R. (1987). *J. Chem. Soc. Perkin Trans. 2* pp. S1–19.

Aly, A. A., Malah, T. E., Ishak, E. A., Brown, A. B. & Elayat, W. M. (2016). *J. Heterocycl. Chem.* **53**, 963–969.

Anchoori, R. K., Kortenhorst, M. S. Q., Hidalgo, M., Sarkar, T., Hallur, G., Bai, R., Diest, P. J. V., Hamel, E. & Khan, S. R. (2008). *J. Med. Chem.* **51**, 5953–5957.

Bielenica, A., Kędzierska, E., Koliński, M., Kmiecik, S., Koliński, A., Fiorino, F., Severino, B., Magli, E., Corvino, A., Rossi, I., Massarelli, P., Kozioł, A. E., Sawczenko, A. & Struga, M. (2016). *Eur. J. Med. Chem.* **116**, 173–186.

Blažek Bregović, V., Basarić, N. & Mlinarić-Majerski, K. (2015). *Coord. Chem. Rev.* **295**, 80–124.

Canatar, C., Türkben, H., Efeoglu, C., Sari, H., Karasu, E., Nural, Y. & Ayaz, F. (2023). *ChemistrySelect* **8**, e202301258.

Etter, M. C., MacDonald, J. C. & Bernstein, J. (1990). *Acta Cryst.* B**46**, 256–262.

Faidallah, H. M., Khan, K. A. & Asiri, A. M. (2011). *J. Fluor. Chem.* **132**, 131–137.

Farrugia, L. J. (2012). *J. Appl. Cryst.* **45**, 849–854.

Groom, C. R., Bruno, I. J., Lightfoot, M. P. & Ward, S. C. (2016). *Acta Cryst.* B**72**, 171–179.

Guang, J., Larson, A. J. & Zhao, J. C. G. (2015). *Adv. Synth. Catal.* **357**, 523–529.

Khan, K. M., Naz, F., Taha, M., Khan, A., Perveen, S., Choudhary, M. & Voelter, W. (2014). *Eur. J. Med. Chem.* **74**, 314–323.

Kumar, V. & Chimni, S. S. (2015). *Anticancer Agents Med. Chem.* **15**, 163–175.

Mackenzie, C. F., Spackman, P. R., Jayatilaka, D. & Spackman, M. A. (2017). *IUCrJ* **4**, 575–587.

Mao, Z., Lin, A., Shi, Y., Mao, H., Li, W., Cheng, Y. & Zhu, C. (2013). *J. Org. Chem.* **78**, 10233–10239.

Mohamed, N. A., Abd El-Ghany, N. A. & Abdel-Aziz, M. M. (2021). *Int. J. Biol. Macromol.* **181**, 956–965.

Oxford Diffraction (2009). *CrysAlis CCD* and *CrysAlis RED*. Oxford Diffraction Ltd, Abingdon, England.

Pingaew, R., Prachayasittikul, V., Anuwongcharoen, N., Prachayasittikul, S., Ruchirawat, S. & Prachayasittikul, V. (2018). *Bioorg. Chem.* **79**, 171–178.

Zhang, Y., Qin, J., Lin, Q. & Wei, T. (2006). *J. Fluor. Chem.* **127**, 1221–1227.

Ribeiro, G. H., Costa, A. R., de Souza, A. R., da Silva, F. V., Martins, F. T., Plutin, A. M. & Batista, A. A. (2023). *Coord. Chem. Rev.* **488**, 215161.

Ruswanto, Miftah, A. M., Tjahjono, D. H. & Siswandono, (2015). *Procedia Chem.* **17**, 157–161.

Saeed, A. & Flörke, U. (2007*a*). *Acta Cryst.* E**63**, o4259.

Saeed, A. & Flörke, U. (2007*b*). *Acta Cryst.* E**63**, o4614.

Saeed, A., Mahmood, S. U., Rafiq, M., Ashraf, Z., Jabeen, F. & Seo, S. Y. (2016). *Chem. Biol. Drug Des.* **87**, 434–443.

Saeed, A., Qamar, R., Fattah, T. A., Flörke, U. & Erben, M. F. (2017). *Res. Chem. Intermed.* **43**, 3053–3093.

Sheldrick, G. M. (2015*a*). *Acta Cryst.* A**71**, 3–8.

Sheldrick, G. M. (2015*b*). *Acta Cryst.* C**71**, 3–8.

Shoukat, N., Rauf, M. K., Bolte, M. & Badshah, A. (2007). *Acta Cryst.* E**63**, o3207.

Singh, R. & Ganguly, S. (2018). *Indian J. Pharm. Educ. Res.* **52**, 655–665.

Spackman, P. R., Turner, M. J., McKinnon, J. J., Wolff, S. K., Grimwood, D. J., Jayatilaka, D. & Spackman, M. A. (2021). *J. Appl. Cryst.* **54**, 1006–1011.

Sultana, S., Khawar Rauf, M., Ebihara, M. & Badshah, A. (2007*a*). *Acta Cryst.* E**63**, o2602.

Sultana, S., Khawar Rauf, M., Ebihara, M. & Badshah, A. (2007*b*). *Acta Cryst.* E**63**, o2801.

Thanigaimalai, P., Lee, K. C., Sharma, V. K., Joo, C., Cho, W. J., Roh, E., Kim, Y. & Jung, S. H. (2011). *Bioorg. Med. Chem. Lett.* **21**, 6824–6828.

Turner, M. J., Thomas, S. P., Shi, M. W., Jayatilaka, D. & Spackman, M. A. (2015). *Chem. Commun.* **51**, 3735–3738.

Ullah, I., Shah, A., Badshah, A., Shah, A., Shah, N. A. & Tabor, R. (2015). *Colloids Surf. A Physicochem. Eng. Asp.* **464**, 104–109.

Xu, S., Li, D., Shaoyong, K. & Liangbin, J. (2003*a*). *Chem. J. Internet* **5**, 67–70.

Xu, X., Qian, X., Li, Z., Huang, Q. & Chen, G. (2003*b*). *J. Fluor. Chem.* **121**, 51–54.

Yusof, M. S. M., Muharam, S. H., Kassim, M. B. & Yamin, B. M. (2008). *Acta Cryst.* E**64**, o1137.

Zhong, Z., Xing, R., Liu, S., Wang, L., Cai, S. & Li, P. (2008). *Carbohydr. Res.* **343**, 566–570.

supporting information

Acta Cryst. (2026). E**82** [https://doi.org/10.1107/S205698902600890X]

Synthesis, crystal structure determination, Hirshfeld surface and crystal void analyses, interaction energy calculations and energy frameworks of *N*-(2-methylphenyl)-*N*′-pivaloylthiourea

Sharatha Kumar and Tuncer Hökelek

Computing details

3-(2,2-Dimethylpropanoyl)-1-(2-methylphenyl)thiourea

Crystal data

$C_{13}H_{18}N_2OS$
$M_r = 250.35$
Triclinic, $P\overline{1}$
$a = 6.1050$ (4) Å
$b = 10.7020$ (3) Å
$c = 11.8910$ (3) Å
$\alpha = 63.290$ (4)°
$\beta = 81.600$ (3)°
$\gamma = 84.340$ (4)°
$V = 686.08$ (6) Å^3
$Z = 2$
$F(000) = 268$
$D_x = 1.212$ Mg m^{-3}
Mo $K\alpha$ radiation, $\lambda = 0.71073$ Å
Cell parameters from 2155 reflections
$\theta = 3.4$–27.7°
$\mu = 0.22$ mm^{-1}
$T = 293$ K
Prism, colourless
0.50 × 0.48 × 0.16 mm

Data collection

Oxford Diffraction Xcalibur with Sapphire CCD Detector diffractometer
Rotation method data acquisition using ω scans.
Absorption correction: multi-scan (*CrysAlis RED*; Oxford Diffraction, 2009)
$T_{min} = 0.897$, $T_{max} = 0.965$
4335 measured reflections
2756 independent reflections
2287 reflections with $I > 2\sigma(I)$
$R_{int} = 0.010$
$\theta_{max} = 26.4°$, $\theta_{min} = 3.4°$
$h = -7\rightarrow7$
$k = -13\rightarrow13$
$l = -10\rightarrow14$

Refinement

Refinement on F^2
Least-squares matrix: full
$R[F^2 > 2\sigma(F^2)] = 0.064$
$wR(F^2) = 0.164$
$S = 1.16$
2756 reflections
160 parameters
3 restraints
Hydrogen site location: mixed
H atoms treated by a mixture of independent and constrained refinement
$w = 1/[\sigma^2(F_o^2) + (0.0561P)^2 + 0.6536P]$ where $P = (F_o^2 + 2F_c^2)/3$
$(\Delta/\sigma)_{max} < 0.001$
$\Delta\rho_{max} = 0.71$ e Å^{-3}
$\Delta\rho_{min} = -0.24$ e Å^{-3}

Special details

Geometry. All esds (except the esd in the dihedral angle between two l.s. planes) are estimated using the full covariance matrix. The cell esds are taken into account individually in the estimation of esds in distances, angles and torsion angles; correlations between esds in cell parameters are only used when they are defined by crystal symmetry. An approximate (isotropic) treatment of cell esds is used for estimating esds involving l.s. planes.

Fractional atomic coordinates and isotropic or equivalent isotropic displacement parameters (Å²)

	x	*y*	*z*	U_{iso}*/U_{eq}
C1	0.6535 (6)	0.0041 (3)	0.7571 (3)	0.0553 (8)
C2	0.4729 (6)	−0.0708 (3)	0.7789 (3)	0.0582 (8)
C3	0.4096 (7)	−0.1702 (4)	0.9074 (3)	0.0694 (10)
H3	0.285478	−0.223253	0.927043	0.083*
C4	0.5310 (8)	−0.1862 (4)	0.9995 (4)	0.0765 (11)
H4	0.486587	−0.250364	1.082242	0.092*
C5	0.7150 (8)	−0.1130 (4)	0.9772 (3)	0.0817 (12)
H5	0.795826	−0.128953	1.043172	0.098*
C6	0.7811 (7)	−0.0141 (4)	0.8549 (3)	0.0712 (10)
H6	0.904989	0.038526	0.837313	0.085*
C7	0.6455 (4)	0.2367 (3)	0.5778 (2)	0.0404 (6)
C8	0.9416 (4)	0.3001 (3)	0.3944 (2)	0.0407 (6)
C9	1.0284 (5)	0.4254 (3)	0.2737 (3)	0.0441 (6)
C10	0.8441 (6)	0.4912 (4)	0.1868 (3)	0.0629 (9)
H10A	0.722387	0.522879	0.229562	0.094*
H10B	0.900447	0.569074	0.110502	0.094*
H10C	0.794361	0.422614	0.165898	0.094*
C11	1.1069 (6)	0.5315 (4)	0.3110 (4)	0.0657 (9)
H11A	0.984175	0.562679	0.353691	0.099*
H11B	1.219945	0.488307	0.366534	0.099*
H11C	1.165792	0.610173	0.236291	0.099*
C12	1.2214 (6)	0.3751 (4)	0.2060 (4)	0.0735 (11)
H12A	1.277779	0.453031	0.129752	0.110*
H12B	1.336465	0.334007	0.260380	0.110*
H12C	1.171636	0.306594	0.185095	0.110*
C13	0.3526 (7)	−0.0550 (4)	0.6784 (4)	0.0762 (10)
H13A	0.230783	−0.116751	0.712468	0.114*
H13B	0.297175	0.039974	0.636992	0.114*
H13C	0.449045	−0.077743	0.618279	0.114*
N1	0.7287 (4)	0.1062 (2)	0.6302 (2)	0.0503 (6)
N2	0.7550 (4)	0.3273 (2)	0.4621 (2)	0.0441 (6)
O1	1.0292 (3)	0.1835 (2)	0.4296 (2)	0.0567 (6)
S1	0.42204 (13)	0.29558 (7)	0.64054 (7)	0.0537 (3)
H1N	0.841 (4)	0.084 (4)	0.592 (3)	0.064*
H2N	0.703 (6)	0.411 (2)	0.434 (3)	0.064*

Atomic displacement parameters (Å²)

	U^{11}	U^{22}	U^{33}	U^{12}	U^{13}	U^{23}
C1	0.066 (2)	0.0377 (14)	0.0473 (16)	0.0103 (13)	0.0110 (14)	−0.0129 (12)
C2	0.066 (2)	0.0470 (16)	0.0556 (18)	0.0094 (15)	0.0014 (15)	−0.0217 (14)
C3	0.084 (3)	0.0492 (18)	0.057 (2)	0.0141 (17)	0.0096 (18)	−0.0166 (16)
C4	0.094 (3)	0.062 (2)	0.055 (2)	0.016 (2)	0.007 (2)	−0.0182 (17)
C5	0.108 (3)	0.074 (2)	0.0485 (17)	0.021 (2)	−0.0178 (19)	−0.0174 (15)
C6	0.093 (3)	0.061 (2)	0.0482 (16)	0.0275 (18)	−0.0149 (17)	−0.0186 (13)
C7	0.0446 (14)	0.0353 (13)	0.0340 (13)	0.0004 (11)	0.0000 (11)	−0.0106 (10)
C8	0.0368 (13)	0.0431 (14)	0.0385 (14)	−0.0004 (11)	−0.0010 (11)	−0.0161 (11)
C9	0.0429 (14)	0.0396 (14)	0.0414 (14)	−0.0011 (11)	0.0065 (11)	−0.0139 (11)
C10	0.072 (2)	0.064 (2)	0.0398 (16)	0.0038 (17)	−0.0042 (15)	−0.0138 (15)
C11	0.059 (2)	0.061 (2)	0.076 (2)	−0.0176 (16)	0.0085 (17)	−0.0317 (18)
C12	0.069 (2)	0.061 (2)	0.066 (2)	0.0026 (17)	0.0296 (17)	−0.0180 (17)
C13	0.082 (3)	0.065 (2)	0.074 (2)	−0.0051 (19)	−0.004 (2)	−0.0240 (19)
N1	0.0527 (14)	0.0404 (12)	0.0407 (13)	0.0072 (11)	0.0092 (11)	−0.0088 (10)
N2	0.0442 (12)	0.0354 (11)	0.0394 (12)	0.0033 (9)	0.0058 (10)	−0.0088 (10)
O1	0.0537 (12)	0.0438 (11)	0.0547 (12)	0.0094 (9)	0.0079 (10)	−0.0123 (9)
S1	0.0573 (5)	0.0395 (4)	0.0482 (4)	0.0048 (3)	0.0144 (3)	−0.0124 (3)

Geometric parameters (Å, º)

C1—C2	1.353 (5)	C9—C12	1.521 (4)
C1—C6	1.424 (5)	C9—C11	1.529 (4)
C1—N1	1.448 (4)	C9—C10	1.536 (4)
C2—C13	1.430 (5)	C10—H10A	0.9600
C2—C3	1.436 (5)	C10—H10B	0.9600
C3—C4	1.350 (6)	C10—H10C	0.9600
C3—H3	0.9300	C11—H11A	0.9600
C4—C5	1.358 (6)	C11—H11B	0.9600
C4—H4	0.9300	C11—H11C	0.9600
C5—C6	1.388 (5)	C12—H12A	0.9600
C5—H5	0.9300	C12—H12B	0.9600
C6—H6	0.9300	C12—H12C	0.9600
C7—N1	1.329 (3)	C13—H13A	0.9600
C7—N2	1.393 (3)	C13—H13B	0.9600
C7—S1	1.665 (3)	C13—H13C	0.9600
C8—O1	1.218 (3)	N1—H1N	0.840 (18)
C8—N2	1.381 (3)	N2—H2N	0.852 (18)
C8—C9	1.525 (4)		
C2—C1—C6	122.8 (3)	C9—C10—H10A	109.5
C2—C1—N1	120.5 (3)	C9—C10—H10B	109.5
C6—C1—N1	116.7 (3)	H10A—C10—H10B	109.5
C1—C2—C13	121.8 (3)	C9—C10—H10C	109.5
C1—C2—C3	117.1 (3)	H10A—C10—H10C	109.5
C13—C2—C3	121.1 (4)	H10B—C10—H10C	109.5

C4—C3—C2	119.7 (4)	C9—C11—H11A	109.5
C4—C3—H3	120.2	C9—C11—H11B	109.5
C2—C3—H3	120.2	H11A—C11—H11B	109.5
C3—C4—C5	123.2 (4)	C9—C11—H11C	109.5
C3—C4—H4	118.4	H11A—C11—H11C	109.5
C5—C4—H4	118.4	H11B—C11—H11C	109.5
C4—C5—C6	119.4 (4)	C9—C12—H12A	109.5
C4—C5—H5	120.3	C9—C12—H12B	109.5
C6—C5—H5	120.3	H12A—C12—H12B	109.5
C5—C6—C1	117.9 (4)	C9—C12—H12C	109.5
C5—C6—H6	121.0	H12A—C12—H12C	109.5
C1—C6—H6	121.0	H12B—C12—H12C	109.5
N1—C7—N2	116.4 (2)	C2—C13—H13A	109.5
N1—C7—S1	124.4 (2)	C2—C13—H13B	109.5
N2—C7—S1	119.26 (19)	H13A—C13—H13B	109.5
O1—C8—N2	121.7 (2)	C2—C13—H13C	109.5
O1—C8—C9	122.8 (2)	H13A—C13—H13C	109.5
N2—C8—C9	115.5 (2)	H13B—C13—H13C	109.5
C12—C9—C8	108.6 (2)	C7—N1—C1	123.3 (2)
C12—C9—C11	110.0 (3)	C7—N1—H1N	119 (2)
C8—C9—C11	108.3 (2)	C1—N1—H1N	117 (2)
C12—C9—C10	109.5 (3)	C8—N2—C7	128.5 (2)
C8—C9—C10	109.9 (2)	C8—N2—H2N	118 (2)
C11—C9—C10	110.5 (3)	C7—N2—H2N	114 (2)

C6—C1—C2—C13	−177.3 (3)	O1—C8—C9—C11	−115.0 (3)
N1—C1—C2—C13	1.3 (5)	N2—C8—C9—C11	65.0 (3)
C6—C1—C2—C3	1.2 (4)	O1—C8—C9—C10	124.2 (3)
N1—C1—C2—C3	179.8 (3)	N2—C8—C9—C10	−55.8 (3)
C1—C2—C3—C4	−0.8 (5)	N2—C7—N1—C1	171.6 (3)
C13—C2—C3—C4	177.7 (3)	S1—C7—N1—C1	−9.1 (5)
C2—C3—C4—C5	−0.6 (6)	C2—C1—N1—C7	84.0 (4)
C3—C4—C5—C6	1.6 (6)	C6—C1—N1—C7	−97.4 (4)
C4—C5—C6—C1	−1.1 (5)	O1—C8—N2—C7	3.5 (5)
C2—C1—C6—C5	−0.3 (5)	C9—C8—N2—C7	−176.5 (3)
N1—C1—C6—C5	−178.9 (3)	N1—C7—N2—C8	−0.8 (4)
O1—C8—C9—C12	4.4 (4)	S1—C7—N2—C8	179.9 (2)
N2—C8—C9—C12	−175.6 (3)		

Hydrogen-bond geometry (Å, º)

*Cg*1 is the centroid of the C1–C6 ring.

D—H···*A*	*D*—H	H···*A*	*D*···*A*	*D*—H···*A*
N1—H1*N*···O1	0.84 (2)	1.98 (3)	2.644 (3)	135 (3)
C11—H11*A*···S1^{i}	0.96	2.79	3.663 (4)	152
C12—H12*C*···*Cg*1^{ii}	0.96	2.92	3.640 (5)	133

Symmetry codes: (i) −*x*+1, −*y*+1, −*z*+1; (ii) −*x*+2, −*y*, −*z*+1.